Summary of April 13, 2016 phone conference and requests from the NP-PWG review committee M. Garcon, S. Kuhn and Zein-Eddine Meziani to M. Hattawy and co-authors

1. RTPC calibration: all previous questions are considered answered satisfactorily. Remains a significant effort to rewrite the corresponding section(s) more clearly.

2. Event selection cuts: the committee acknowledges the numerous studies (variation of cuts) that have been performed. It is not fully convinced, however, that there is no remaining background (other than π^0s only) in either channel, and about the argument on the statistics (for cutting tails). Consequently, it is requested:

   (a) To show plots of correlations between exclusivity cuts:

      i. 2D missing $ep\gamma X$ M2 vs $\Delta\phi$: is there a gain to be expected by a contour cut? If yes, implement.
      The results are shown in figure 1 before and after the exclusivity cuts. No clear dependence is observed.

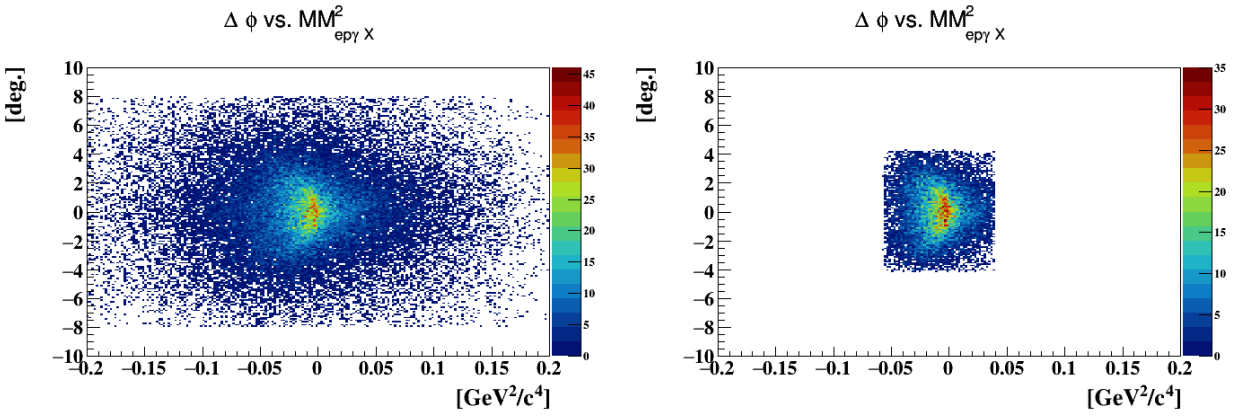

Figure 1: $\Delta\phi$ vs. $MM^2_{ep\gamma X}$ before (left) and after (right) the exclusivity cuts.

      ii. Produce all 9 plots in right figure of slides 5 and 9 of `https://clasweb.jlab.org/rungroups/lowq/wiki/images/a/a0/ExcluCuts-CANeg6.pdf` for a 2σ and 1σ cuts on missing $ep\gamma X$ M2.
      The coherent and the incoherent distributions are presented in figure 2 and 4 respectively. The reconstructed coherent and incoherent beam spin asymmetries are presented in figures 3 and 5 respectively. In terms of the exclusivity distributions, no correlations were observed in the coherent DVCS channel, while a slight correlation was observed between the $ep\gamma$ MM2 and epX MM2.

   (b) (optionally) In the incoherent case, extract ALU with 2 variations of the ep missing M2 right cut, moving it tighter to the left (e.g. 1 and 0.75 GeV2). (also see the evolution of the other distributions when doing so).
   The reconstructed incoherent asymmetries are presented in figure 6 with the associated exclusive distributions in figure 7. We conclude that the different tail cuts show no major effects on the reconstructed A_{LU}.

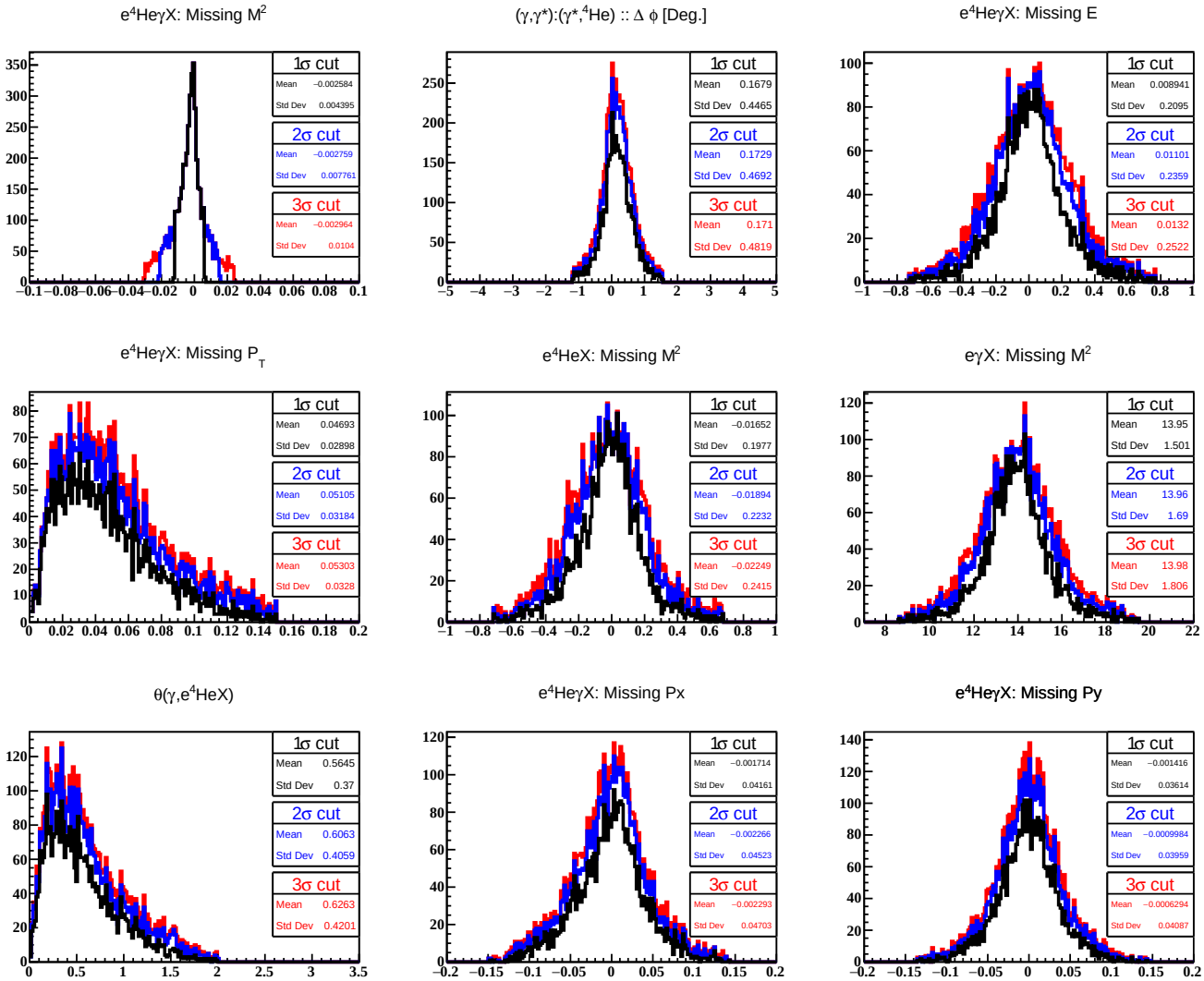

Figure 2: Coherent exclusivity distributions corresponding to different cuts on $e^4He\gamma X$ missing mass squared.

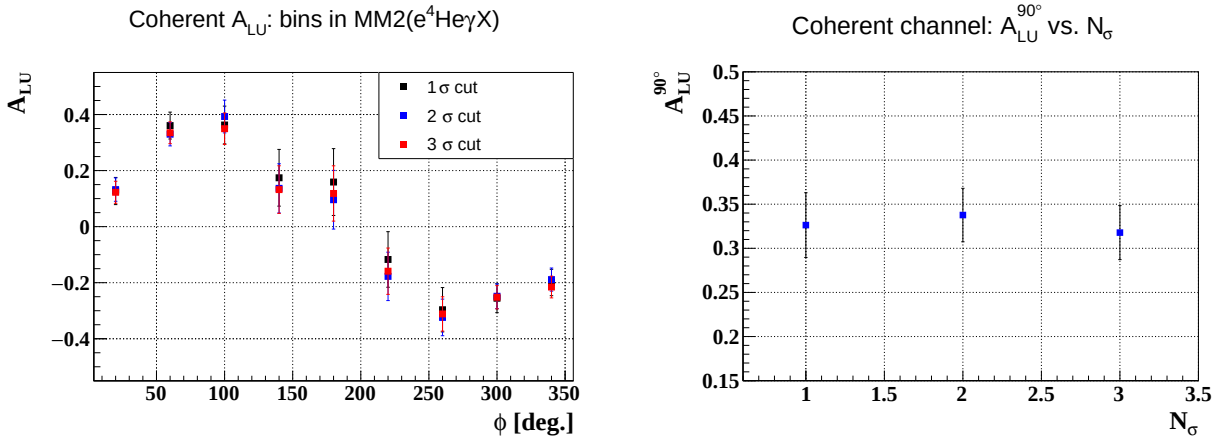

Figure 3: On the left: the integrated coherent beam-spin asymmetries as a function of ϕ corresponding to different cuts on $e^4He\gamma X$ missing mass squared. On the right: A_{LU} at 90° from fitting the reconstructed asymmetries as a function of the cut width.

3. Free proton asymmetries from FX's publication: implement a (possibly 3D/9 points) interpolation to smooth out both statistical fluctuations and kinematical dependences. Reintroduce a corresponding section in the CAN. Take into account both stat. and syst. errors of both experiments in the ratio. The committee recommends though to be cautious about the statements on the asymmetry ratios in the future publication.
   We changed the procedures completely, see Appendix G in the latest version of the analysis note. We performed fittings for the published free proton asymmetries. Then we used those fits to extrapolate the free proton asymmetries at our measured kinematics.

4. CFF: the committee acknowledges that the new procedure (2-parameter fit with complete formula at leading-twist) is more satisfying. It recommends though to be cautious about the statements on CFF in the future publication.

5. CAN: a number of answers to previous questions have to appear in the CAN. This includes (but may not be limited to)

   Figs 1-4 of `https://clasweb.jlab.org/rungroups/lowq/wiki/images/a/a3/Final_1st_round_comments.pdf` Tighter *edist* cut [-2,+3 mm]. Otherwise, even if you do not show it in the CAN, mention in one line that a specific study was done.
   The analysis note has been updated with all the required plots. See Q.7 for the new updates in the note.

6. Miscellaneous:

   (a) 4-D dependences of the ratio R: the statement that the integrated R's are flat is disputable (see Figs 4.16 and 4.17), but we are ready to accept that the effect discussed is small and taken care of in the systematic errors.
   We implemented a 4D ratio R for the background subtraction. The difference between the reconstructed ALU with 2D and 4D background subtraction are presented in figures 11 and 12 for the coherent and the incoherent DVCS channels. Even though the 2D was a good approximation, a 4D subtraction is applied on the final results.

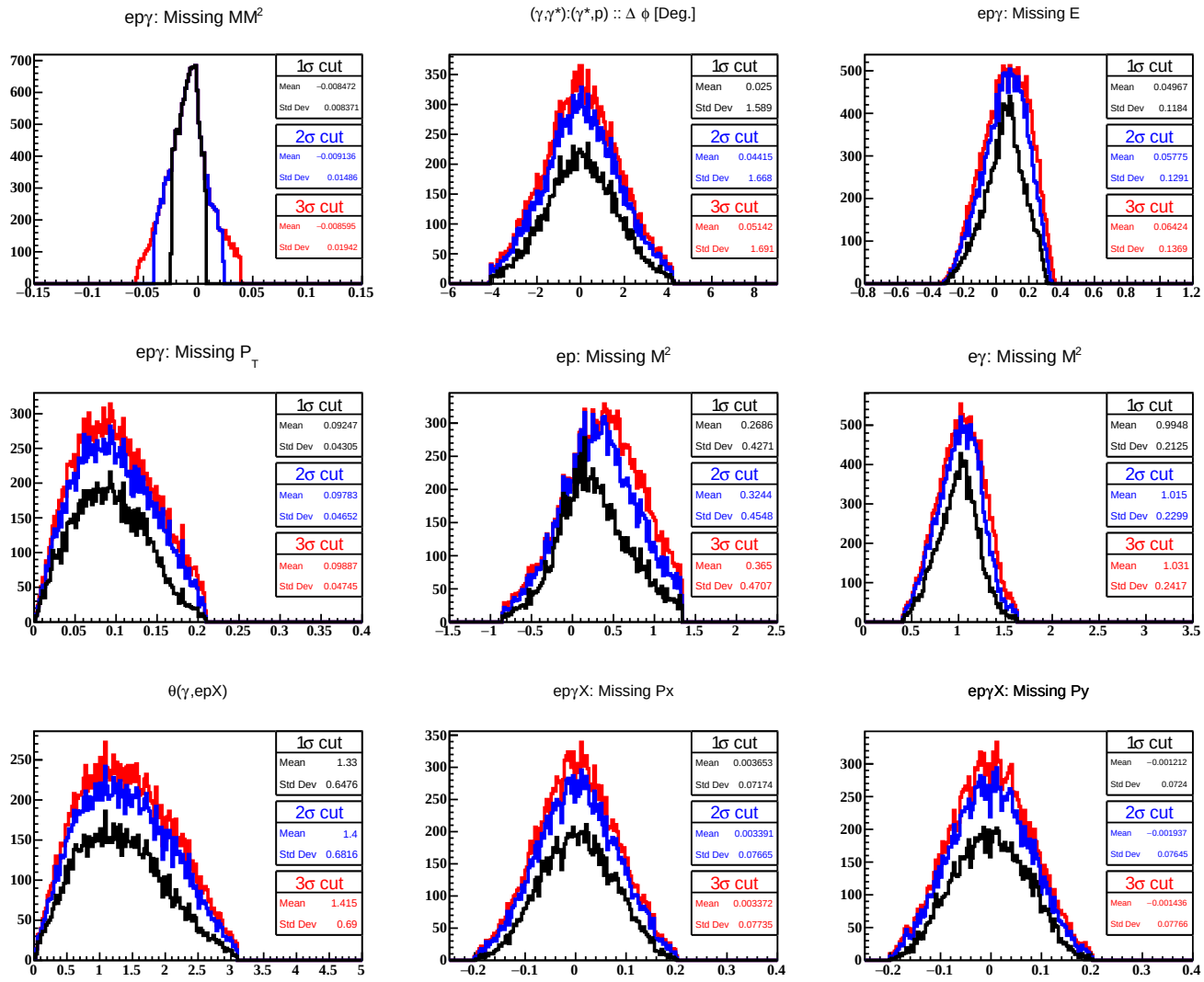

Figure 4: Incoherent exclusivity distributions for the different cuts on $ep\gamma X$ missing mass squared.

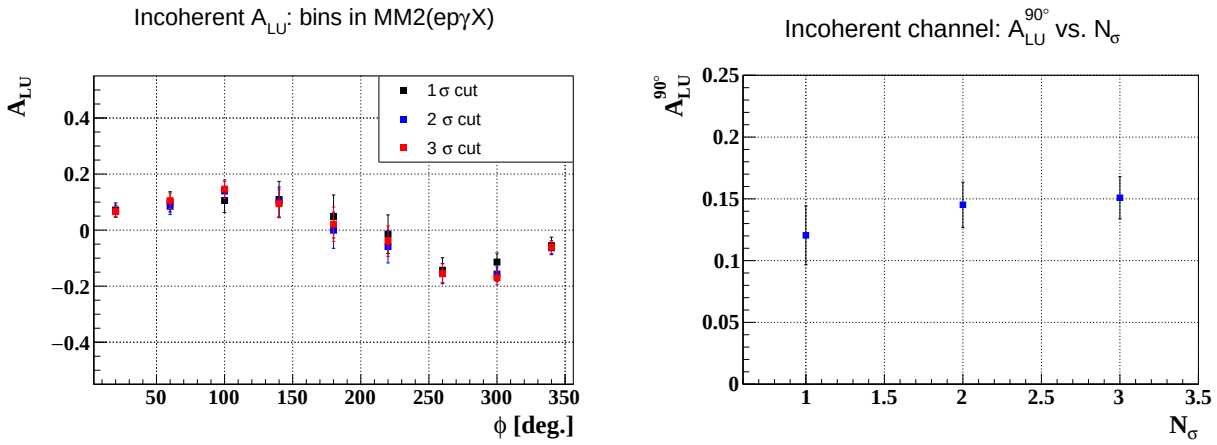

Figure 5: On the left: the integrated incoherent beam-spin asymmetries as a function of ϕ corresponding to different cuts on $e^4He\gamma X$ missing mass squared. On the right: A_{LU} at 90° from fitting the reconstructed asymmetries as a function of the cut width.

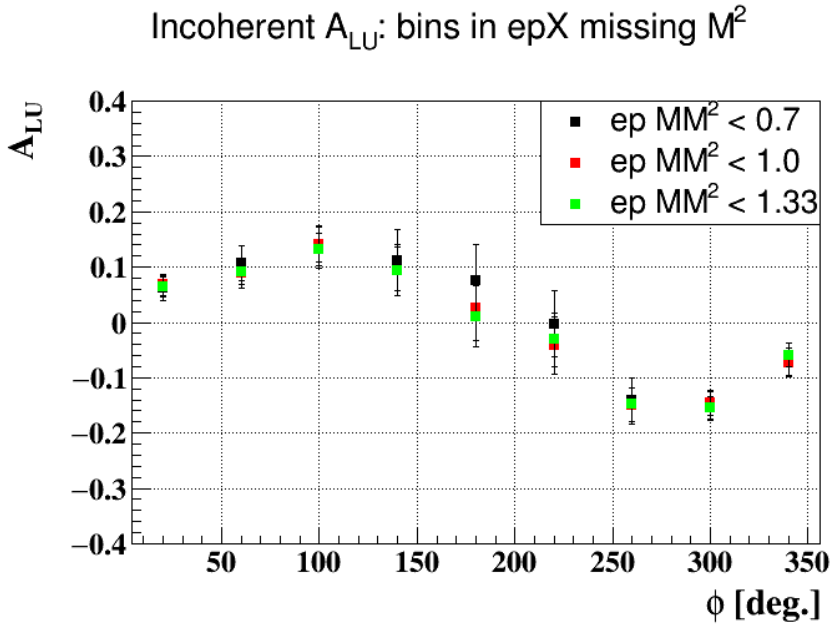

Figure 6: The integrated, over Q^2, x_B, and $-t$, incoherent beam-spin asymmetries as a function of ϕ for the different cuts on epX missing mass squared.

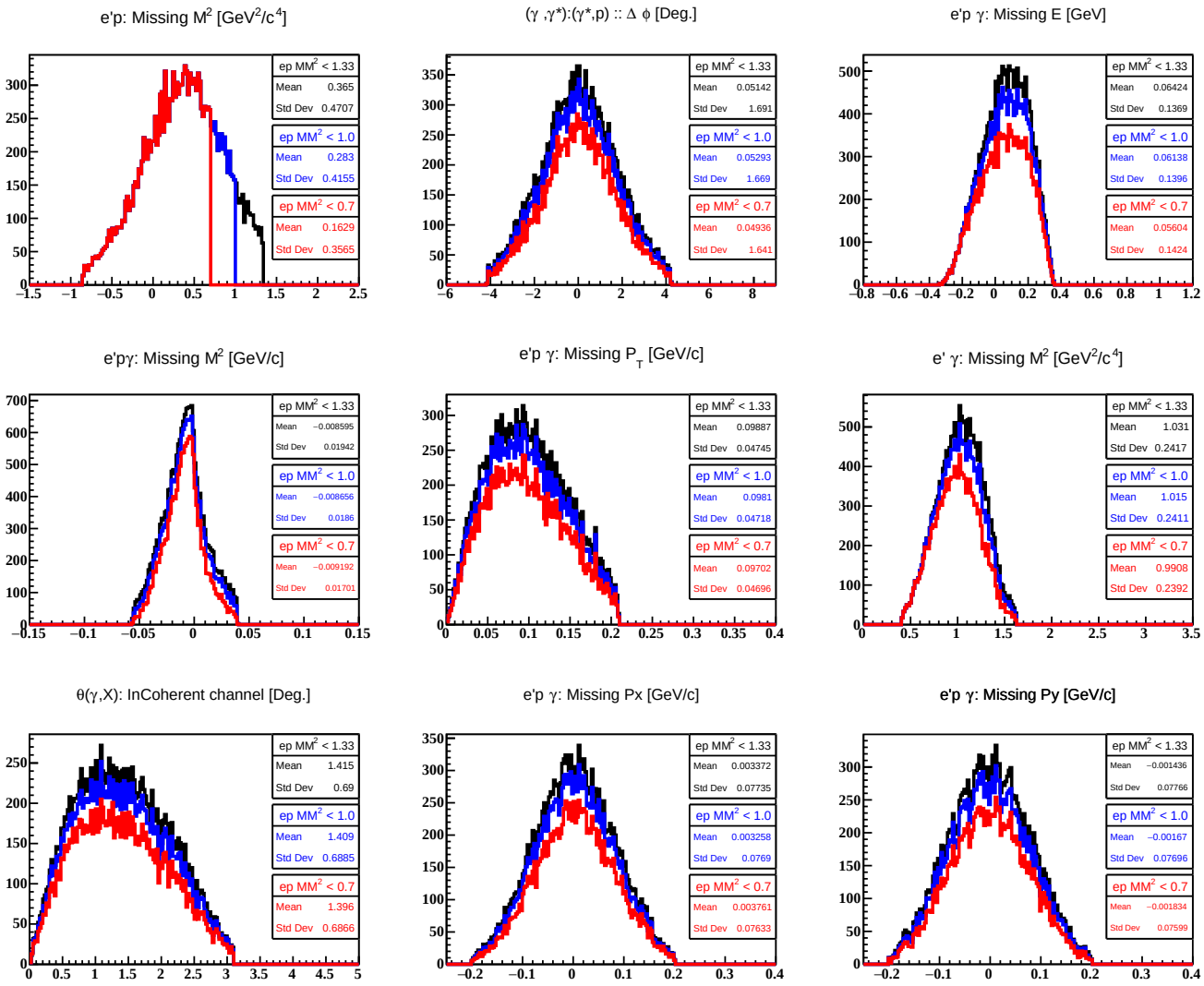

Figure 7: Incoherent exclusivity distributions for the different cuts on epX missing mass squared.

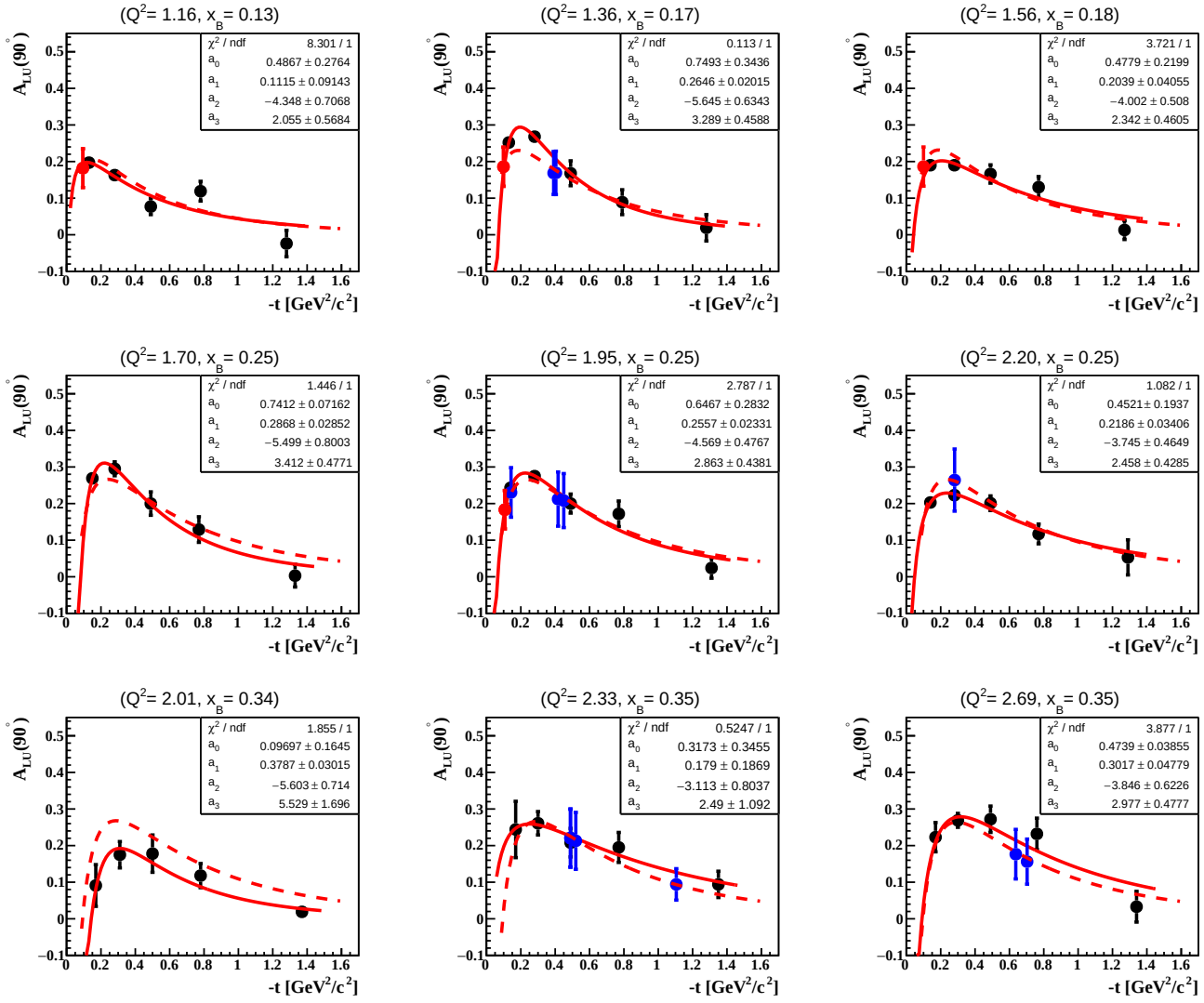

Figure 8: Black circles are the free proton beam-spin asymmetries at $\phi = 90^\circ$ as a function of $-t$ in different (x_B, Q^2) bins as measured at CLAS-E1DVCS experiment. The solid red curves are fits to the free proton asymmetries in the form $a_0 * (\sqrt{t} - a_1) * e^{a_2 * \sqrt{t} - a_3}$. The dashed curves are calculations using the fitted a_i's parameters as a function of x_B. Blue points are the interpolated points corresponding for the incoherent points presented in this analysis. The red points stand for the extrapolated free proton asymmetries at the measured coherent kinematics.

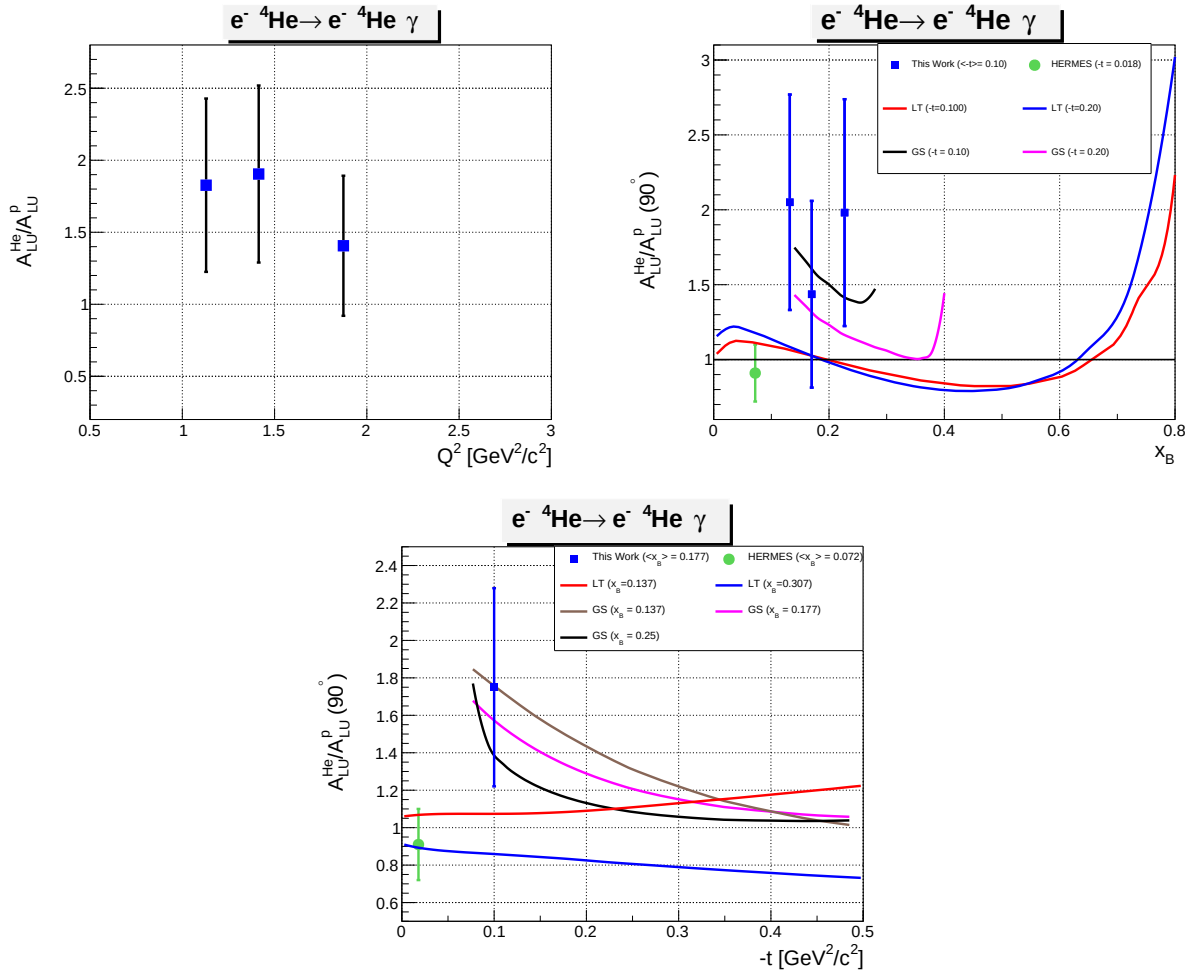

Figure 9: A_{LU} ratio between ^{4}He DVCS and free proton at $\phi = 90^\circ$ as a function of Q^2, x_B, and $-t$.

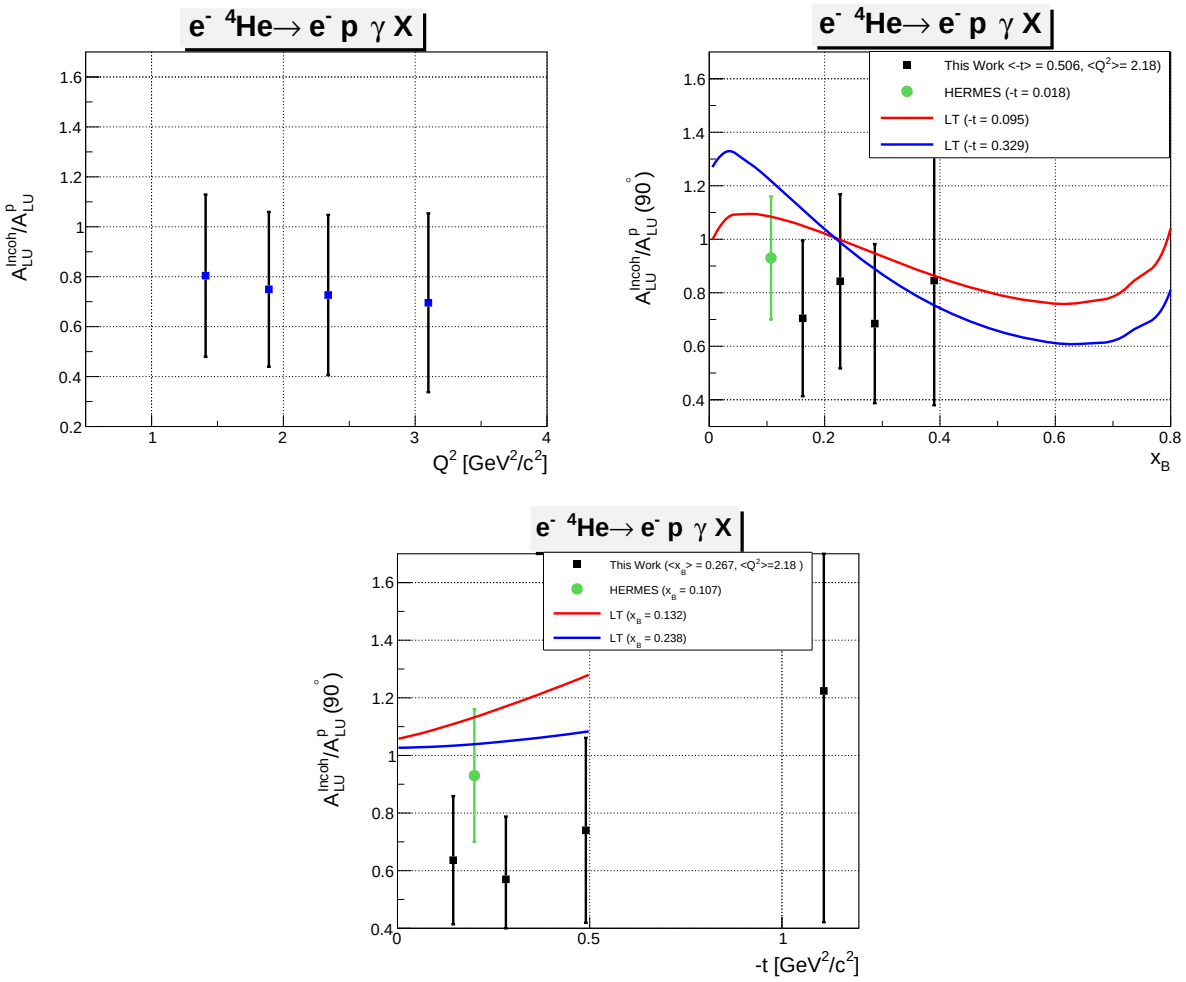

Figure 10: A_{LU} ratio between bound proton and free proton at $\phi = 90^\circ$ as a function of Q^2, x_B, and $-t$.

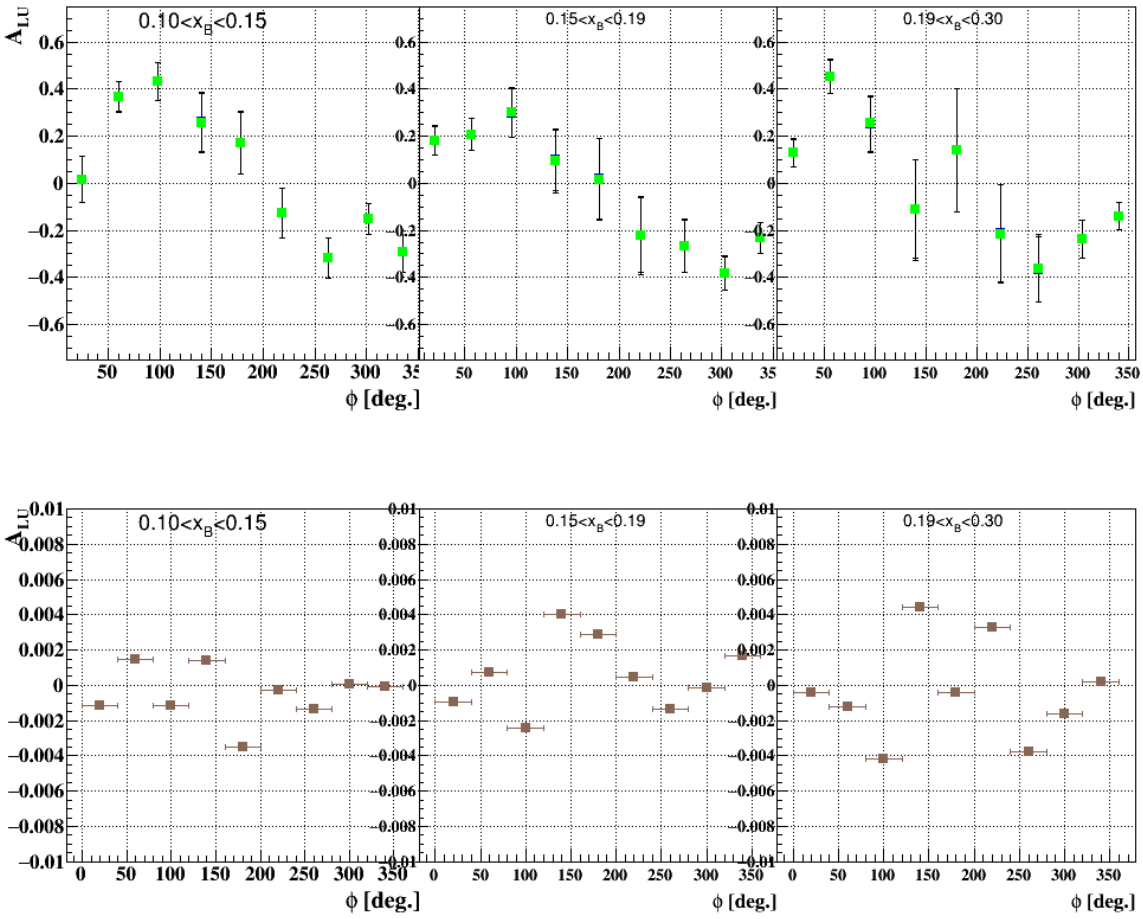

Figure 11: On top: the reconstruct coherent beam-spin asymmetries as a function of ϕ in x_B bins using 2D (in blue) and 4D (in green) background subtraction. On bottom: the difference between the two asymmetries as a function of ϕ.

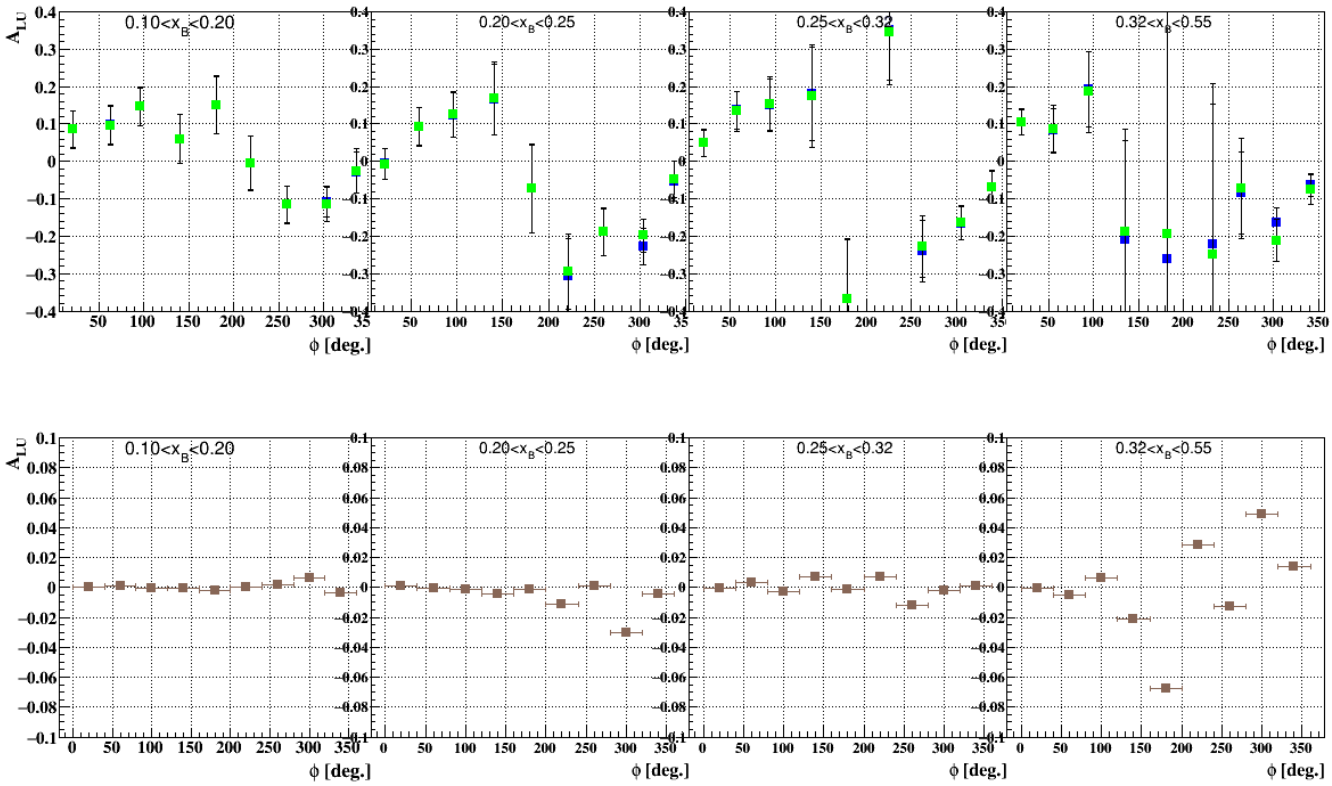

Figure 12: On top: the reconstruct incoherent beam-spin asymmetries using 2D (in blue) and 4D (in green) background subtraction. On bottom: the difference between the two asymmetries as a function of ϕ.

(b) not convinced that comparing 9 phi-bins to 11 is a definitive answer, when not applying any finite bin size correction. But again, in view of the size of statistical and systematic errors, would accept that.

(c) Your Eq.(4) of "answer" is probably wrong. For our own understanding, look into this argument again.
Sorry there was a missig sign. This is the correct dependence.

$$\frac{\partial MM^2_{e\gamma X}}{\partial E_\gamma} = -2 * (E_{\gamma^*} + M_{target} - E_\gamma) \tag{1}$$

7. Please keep a record of the changes in the CAN, as we will probably not re-read the whole text.

(a) Added the run conditions section 1.2.4.

(b) Updated figure 2.2.

(c) Update section 2.1.3 Track reconstruction.

(d) Update section 2.2.1.1

(e) Added section 2.2.1.3 Checking the initial good track requirements.

(f) Cleaning section 2.2.2 with adding a summary for the drift paths and the drift speed calibrations, section 2.2.2.3

(g) Cleaning section 2.2.3 Gain calibration with adding more demanded plots.

(h) Added section 2.4 RTPC efficiency.

(i) Cleaned section 3.2.5 with adding the required plots.

(j) Added the demanded plots in section 4.1.2 and cleaning the writing.

(k) Added a new section 4.1.3 regarding checking the selected coherent DVCS events.

(l) Edited the plots in figure 4.15 with the -tmin lines.

(m) Cleaning section 4.5 after changing to perform 4D background subtraction with a summery about other background sources and a new section for the accidental contaminations.

(n) Updated section 4.7 Systematic uncertainties with all suggested studies.

(o) Updated section 5.1 with the new fitting procedures for the coherent channel.

(p) Updated all the figure in chapter 5 with the new results and the suggested modifications.

(q) Added Appendix F with A_{LU} tables.

(r) Added Appendix G for the free proton asymmetry interpolations.

8. Request to see the very first draft of the publication. Will be provided.